

# The $C^1\Pi_u$ and $2^1\Sigma_u^+$ states in $Li_2$ : Experiment and comparison with theory

M.K. Kubkowska<sup>a</sup>, A. Grochola<sup>a</sup>, W. Jastrzebski<sup>b</sup>, P. Kowalczyk<sup>a,\*</sup>

<sup>a</sup> *Institute of Experimental Physics, Warsaw University, ul. Hoża 69, 00-681 Warsaw, Poland*

<sup>b</sup> *Institute of Physics, Polish Academy of Sciences, Al. Lotników 32/46, 02-668 Warsaw, Poland*

Received 20 December 2006; accepted 7 February 2007

Available online 9 February 2007

## Abstract

The  $C^1\Pi_u$  and  $2^1\Sigma_u^+$  states of lithium dimer are investigated experimentally by polarization labelling spectroscopy. The inverted perturbation approach method is used to construct the potential energy curves of both states. A very good agreement is found between the experimental potentials and those resulting from the most recent theoretical calculations.

© 2007 Elsevier B.V. All rights reserved.

PACS: 31.50.Df; 33.20.Kf; 33.20.Vq; 42.62.Fi

Keywords: Diatomic molecules; Electronic states; Potential energy curves; Laser spectroscopy

## 1. Introduction

Investigations of electronic structure of the lithium dimer are of primary importance, because it is the smallest stable homonuclear diatomic molecule beside  $H_2$ . As such, it allows high quality calculations of its properties and, fortunately, is also relatively easy to handle experimentally. Recent calculations by Jasik and Sienkiewicz [1] provide potential energy curves for 25 electronic states and claim very high accuracy but this work contains surprisingly few comparisons with experimental results. Indeed, though experimental studies of  $Li_2$  are numerous and include observation of such subtle effects as breakdown of the Born–Oppenheimer approximation [2] or nonadiabatic mixing of electronic states of gerade and ungerade inversion symmetry [3], but of the singlet ungerade states only  $A^1\Sigma_u^+$  and  $B^1\Pi_u$  have been thoroughly investigated. Even the next two states of singlet ungerade symmetry,  $2^1\Sigma_u^+$  and  $C(2)^1\Pi_u$ , are less known, in particular the potential curve for the C state had been determined reliably only

around its minimum [4]. The main aim of the present work was therefore to extend the range of experimentally observed rovibrational levels in the  $C^1\Pi_u$  state and to improve the quality of the molecular potential with a final objective of further verification of the theoretical results reported in Ref. [1]. In addition, we have recorded transitions to levels of the double minimum  $2^1\Sigma_u^+$  state higher than reported before [4] which also allowed for extension of the corresponding potential energy curve and provided a further sensitive test of theoretical predictions. In the following sections, we present the experimental apparatus and procedure, describe the construction of the potential energy curves from the measured spectra and finally compare them with the theoretical ones.

## 2. Experimental

To study the  $C^1\Pi_u \leftarrow X^1\Sigma_g^+$  and  $2^1\Sigma_u^+ \leftarrow X^1\Sigma_g^+$  band systems, we used the V-type optical–optical double resonance polarization labelling spectroscopy technique with two independent pump and probe lasers. Only a brief outline of the experimental arrangement is given here as a detailed description can be found elsewhere [5,6]. In our

\* Corresponding author. Tel.: +48 22 5532249; fax: +48 22 6210985.  
E-mail address: [pfkowal@fuw.edu.pl](mailto:pfkowal@fuw.edu.pl) (P. Kowalczyk).

version of the method the probe laser had a fixed frequency and excited a few known molecular transitions, while the pump laser was tuned over an investigated spectrum. The pump light was generated by a parametric oscillator/amplifier system (OPO/OPA, Sunlite Ex, Continuum) equipped with a frequency doubler (FX-1) and pumped with the third harmonic of an injection seeded Nd:YAG laser (Pow-erlite 8000). The system generated pulsed UV radiation with a typical energy of 5 mJ, 10 ns duration and  $0.16 \text{ cm}^{-1}$  spectral width, tuneable for purposes of the present experiment in the range  $28,900\text{--}33,800 \text{ cm}^{-1}$ . Wave number calibration was achieved by taking optogalvanic spectra of argon and by additional sampling of the pump light with a  $0.5 \text{ cm}$  long Fabry–Pérot interferometer (both auxiliary signals being observed at a fundamental frequency of tuneable OPO/OPA radiation). The accuracy of measured laser wave numbers was estimated as better than  $0.1 \text{ cm}^{-1}$ . As sources of the probe (labelling) light we used the following lasers: Ar<sup>+</sup>–Kr<sup>+</sup> (Carl Zeiss ILM 120,  $\lambda = 476.5, 488.0, 496.5, 501.7, 514.5$  or  $647.1 \text{ nm}$ ,  $20\text{--}200 \text{ mW}$ ), He–Ne (Carl Zeiss HNA 188-1,  $\lambda = 632.8 \text{ nm}$ ,  $30 \text{ mW}$ ), or a home built pulsed dye laser (Shoshan-type design [7], spectral width about  $1 \text{ cm}^{-1}$ , pumped synchronously by the Nd:YAG laser) operated on chosen wavelengths between  $630$  and  $650 \text{ nm}$  (DCM dye). At all the employed wavelengths, the probe beam excited transitions in the  $A^1\Sigma_u^+ \leftarrow X^1\Sigma_g^+$  or  $B^1\Pi_u \leftarrow X^1\Sigma_g^+$  systems of Li<sub>2</sub>, easy to assign with the well known molecular constants of the X, A and B states [8,9]. Table 1 presents a summary of all the identified labelling transitions induced by the probe lasers, which gave rise to the polarization spectra. The Li<sub>2</sub> molecules were prepared in a stainless steel heat pipe oven by heating metallic lithium (natural isotopic composition) to  $770 \text{ }^\circ\text{C}$  with  $5 \text{ mbar}$  of helium as a buffer gas. The pump and probe laser beams were copropagated through the centre of the heat pipe. Crossed polarizers were placed at both sides of the oven in the path of the probe beam. At these frequencies, at which transitions induced by the pump beam shared the same lower level with any of the probe transitions, some of the probe light passed through the analyzer. This residual beam was monitored with a photomultiplier tube connected to the boxcar averager (Stanford Research Systems, SR250). The polarization spectra were stored in a computer along with the reference optogalvanic spectra and frequency markers of the interferometer. The same computer was used simultaneously to control tuning of the OPO/OPA system.

### 3. Measurements and data analysis

As the spectroscopic constants describing the lowest levels of the  $C^1\Pi_u$  state were known [4], it was relatively easy to identify 30 vibrational progressions in the  $C^1\Pi_u \leftarrow X^1\Sigma_g^+$  band system of lithium dimer (26 of them in  $^7\text{Li}_2$  and 4 in  $^6\text{Li}^7\text{Li}$ ), in their parts corresponding to low  $v'$  values in the C state. Subsequently, we were able to follow them up step by step, reaching higher vibrational

Table 1

Observed transitions in the  $A^1\Sigma_u^+ \leftarrow X^1\Sigma_g^+$  and  $B^1\Pi_u \leftarrow X^1\Sigma_g^+$  systems of Li<sub>2</sub> excited by the probe (labelling) lasers

Laser wave number	Labelled transition
20981.1 $\text{cm}^{-1}$ (Ar <sup>+</sup> 476.5 nm)	$B(v' = 4, J' = 24) \leftarrow X(v'' = 1, J'' = 24)$
20486.7 $\text{cm}^{-1}$ (Ar <sup>+</sup> 488.0 nm)	$B(v' = 1, J' = 32) \leftarrow X(v'' = 0, J'' = 33)$ $B(v' = 1, J' = 37) \leftarrow X(v'' = 0, J'' = 37)$ $B(v' = 2, J' = 31) \leftarrow X(v'' = 1, J'' = 30)$
20135.0 $\text{cm}^{-1}$ (Ar <sup>+</sup> 496.5 nm)	$B(v' = 0, J' = 47) \leftarrow X(v'' = 0, J'' = 47)$ $B(v' = 0, J' = 45) \leftarrow X(v'' = 0, J'' = 45)^*$
19926.0 $\text{cm}^{-1}$ (Ar <sup>+</sup> 501.7 nm)	$B(v' = 0, J' = 33) \leftarrow X(v'' = 1, J'' = 33)$ $B(v' = 1, J' = 20) \leftarrow X(v'' = 2, J'' = 20)$
19429.8 $\text{cm}^{-1}$ (Ar <sup>+</sup> 514.5 nm)	$B(v' = 2, J' = 30) \leftarrow X(v'' = 4, J'' = 31)$
15798.0 $\text{cm}^{-1}$ (He–Ne 632.8 nm)	$A(v' = 14, J' = 42) \leftarrow X(v'' = 3, J'' = 43)$
15449.6 $\text{cm}^{-1}$ (Kr <sup>+</sup> 647.1 nm)	$A(v' = 9, J' = 11) \leftarrow X(v'' = 2, J'' = 12)$
Dye laser:	
15813.5 $\text{cm}^{-1}$	$A(v' = 12, J' = 3) \leftarrow X(v'' = 3, J'' = 4)$ $A(v' = 12, J' = 9) \leftarrow X(v'' = 3, J'' = 8)$
15794.0 $\text{cm}^{-1}$	$A(v' = 12, J' = 8) \leftarrow X(v'' = 3, J'' = 9)$ $A(v' = 12, J' = 14) \leftarrow X(v'' = 3, J'' = 13)$ $A(v' = 9, J' = 24) \leftarrow X(v'' = 1, J'' = 23)^*$
15740.8 $\text{cm}^{-1}$	$A(v' = 12, J' = 16) \leftarrow X(v'' = 3, J'' = 17)$ $A(v' = 12, J' = 22) \leftarrow X(v'' = 3, J'' = 21)$
15737.6 $\text{cm}^{-1}$	$A(v' = 15, J' = 39) \leftarrow X(v'' = 4, J'' = 40)$ $A(v' = 15, J' = 20) \leftarrow X(v'' = 5, J'' = 19)$ $A(v' = 9, J' = 23) \leftarrow X(v'' = 1, J'' = 24)^*$
15534.2 $\text{cm}^{-1}$	$A(v' = 8, J' = 15) \leftarrow X(v'' = 1, J'' = 16)$ $A(v' = 10, J' = 26) \leftarrow X(v'' = 2, J'' = 27)$ $A(v' = 6, J' = 3) \leftarrow X(v'' = 0, J'' = 4)^*$
15482.8 $\text{cm}^{-1}$	$A(v' = 6, J' = 2) \leftarrow X(v'' = 0, J'' = 3)$ $A(v' = 6, J' = 8) \leftarrow X(v'' = 0, J'' = 7)$ $A(v' = 9, J' = 10) \leftarrow X(v'' = 2, J'' = 9)$
15410.0 $\text{cm}^{-1}$	$A(v' = 6, J' = 16) \leftarrow X(v'' = 0, J'' = 17)$ $A(v' = 10, J' = 41) \leftarrow X(v'' = 2, J'' = 40)$ $A(v' = 11, J' = 27) \leftarrow X(v'' = 3, J'' = 28)$

The stars indicate excitation of  $^6\text{Li}^7\text{Li}$ , otherwise  $^7\text{Li}_2$  was excited.

levels. In this way over 1000 transitions were assigned in the  $C \leftarrow X$  system, spanning the range  $0 \leq v' \leq 21$ ,  $2 \leq J' \leq 48$ . However, several (usually weaker) spectral lines were clearly not belonging to this system. Most of them also formed progressions, characterized by substantially smaller vibrational and rotational spacings and by the absence of  $Q$  lines. We attributed them to transitions from the ground state of Li<sub>2</sub> to rovibrational levels of the double minimum  $2^1\Sigma_u^+$  state located above the potential barrier. Again for assignment of the least energetic transitions we could use the potential energy curve of the  $2^1\Sigma_u^+$  state [4] but the range of observed levels ( $v' \leq 50$ ) exceeded that reported previously. In the following two subsections, we present separately our analysis related to each of the two excited states.

#### 3.1. The $C^1\Pi_u$ state

At closer inspection of the  $C^1\Pi_u \leftarrow X^1\Sigma_g^+$  spectra, the patterns of the  $P$ ,  $Q$  and  $R$  lines in the observed progressions turn out to be irregular. This is not surprising as a

perturbation of the C state by the  $2^1\Sigma_u^+$  state is well known [4]. Since this perturbation affects only positions of *e* parity levels (accessed through *P* and *R* lines in the spectra), we have limited our analysis of the  $C^1\Pi_u$  state to levels of *f* parity, observed via *Q* lines. For reasons discussed below, the analysis has been confined to the  $^7\text{Li}_2$  isotopomer, giving rise to a major part of the recorded spectra. The known term energies of the labelled ground state levels [8] were added to transition wave numbers to obtain term values  $T(v', J')$  of rovibronic levels in the C state, referred to the bottom of the ground state potential well. In addition to the levels observed in the present experiment, 79 *f* parity levels related to  $v' = 0, 1, 2, 4$  and 5 from previous works by Ross et al. [10] and Kasahara et al. [4], were also included to the analysis. The input data thus defined (Fig. 1) consists of energies of 398 rovibronic levels and fills very well the investigated range of  $v'$  and  $J'$  quantum numbers. At the initial stage of the analysis these term values were subjected to a least-squares fit with a Dunham expansion

$$T(v', J') = T_e + \sum_{i,k} Y_{ik} (v' + 0.5)^i [J'(J' + 1) - 1]^k, \quad (1)$$

where the symbols  $T_e$  and  $Y_{ik}$  have their usual meaning. However, although many fits have been made for varying numbers of Dunham coefficients, all of them proved inadequate for precise description of the lowest vibrational levels in the  $C^1\Pi_u$  state,  $v' = 0-2$ , providing discrepancies exceeding  $1 \text{ cm}^{-1}$ . To check whether this is a result of additional perturbation, affecting *f* parity levels, or rather a numerical artifact arising from a specific shape of the molecular potential, we have examined an alternative possibility to describe the C state directly by its potential curve constructed by the pointwise inverted perturbation approach (IPA) method [11]. The method is based on iterative optimization of an estimated initial potential in such a way

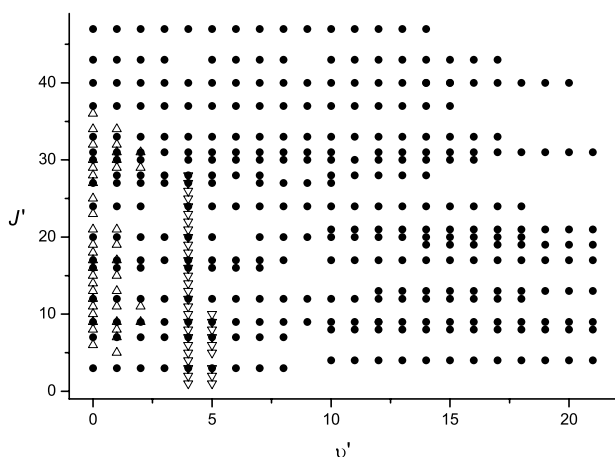


Fig. 1. Distribution of the experimental data (related to *f* parity levels) in the field of vibrational and rotational quantum numbers of the  $C^1\Pi_u$  state in  $^7\text{Li}_2$ , originating from this investigation (full circles) as well as from the works by Kasahara et al. [4] (down triangles) and Ross et al. [10] (up triangles).

that the calculated eigenenergies agree in a least-squares sense with the experimental term values. As the input curve we used an RKR curve based on one of the “imperfect” sets of Dunham coefficients for the C state, extended smoothly to small and large *R* values with the theoretical potential [1]. It turned out that after a few iterations the potential energy curve was generated, which reproduces the energies of all 398 observed *f* parity rovibrational levels with a standard deviation  $0.05 \text{ cm}^{-1}$ , consistent with the precision of the measurements. We conclude then that within the observed range of vibrational and rotational quantum numbers the *f* parity levels in the C state are free of perturbation and that we encounter here an example of a potential which, albeit regular in shape, is unsuitable for representation by means of a power series in  $R - R_e$  (at least by a series containing relatively small number of terms). The shape of the potential curve (Fig. 2) with its rather unusual, nearly linear part between 4.0 and 5.8 Å in the outer wall, may explain this finding. The IPA potential energy curve of the  $C^1\Pi_u$  state is defined uniquely by 23 points (Table 2) together with the natural spline procedure [12] to be used for interpolation of the potential at any arbitrary point. To obtain the quoted accuracy of level positions, the Schrödinger equation has to be solved in a mesh of at least 7000 points between 1.8 and 9.8 Å. The error analysis specific to the pointwise IPA method [13] shows that, with the input data used in the present work, the potential curve is determined reliably between ca. 2.2 and 5.4 Å, i.e., approximately up to the energy of  $35,000 \text{ cm}^{-1}$  on the rotationless potential. In this range, the statistical errors of points defining the potential and listed in Table 2 are  $\pm 0.1 \text{ cm}^{-1}$ . Points of the potential outside of the range given above have to be provided in order

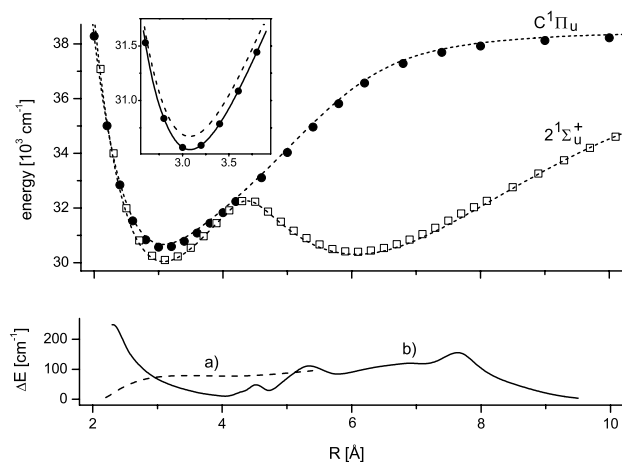


Fig. 2. Upper part: The pointwise IPA potential energy curves of the  $C^1\Pi_u$  state (full circles, in the inset connected with a solid line) and  $2^1\Sigma_u^+$  state (open squares) compared with the calculations of Jasik and Sienkiewicz [1] (dashed lines). The inset shows the region around the potential minimum of the  $C^1\Pi_u$  state. Lower part: Differences between the experimental and theoretical potentials for (a) the  $C^1\Pi_u$  state,  $E_{\text{theor}} - E_{\text{exp}}$ , and (b) the  $2^1\Sigma_u^+$  state,  $E_{\text{exp}} - E_{\text{theor}}$ , displayed in the range where the experimental potentials are determined reliably.

Table 2  
The rotationless IPA potential energy curve of the  $C^1\Pi_u$  state in  ${}^7\text{Li}_2$

$R$ (Å)	$V$ ( $\text{cm}^{-1}$ )	$R$ (Å)	$V$ ( $\text{cm}^{-1}$ )
1.8	42760.6283	4.2	32235.6985
2.0	38287.2103	4.6	33104.4104
2.2	35005.8120	5.0	34033.0434
2.4	32842.6971	5.4	34961.1174
2.6	31530.5193	5.8	35819.5130
2.8	30836.5225	6.2	36565.9696
3.0	30570.6673	6.8	37287.0995
3.2	30589.0755	7.4	37694.1332
3.4	30786.2277	8.0	37923.6388
3.6	31087.3410	9.0	38127.4031
3.8	31443.8045	10.0	38223.2947
4.0	31829.8078		

Note: The potential minimum is located at  $T_e = 30550.52 \text{ cm}^{-1}$  and corresponds to  $R_e = 3.081 \text{ Å}$ .

to secure proper boundary conditions for solving the radial Schrödinger equation but, due to the properties of the cubic spline interpolation, they also have some influence on the inner part of the potential. For the readers' convenience an alternative way to describe the  $v' = 0\text{--}21$  levels in the C state in a form of band-by-band constants is provided as [Supplementary material](#). It must be noted that in case of  $e$  parity levels, the potential curve given here may serve only for a rough prediction of their positions and the energy mismatch between the calculated and measured energies can exceed  $2 \text{ cm}^{-1}$ , particularly for higher  $J'$  values.

The C state dissociates to a pair of Li(2p) atoms with a combination of fine structure components  $2^2P_{1/2} + 2^2P_{3/2}$  [10]. Using the ground state dissociation energy ( $8516.61 \pm 0.08 \text{ cm}^{-1}$  [14,15]), the Li atomic excitation energies ( $E(2^2P_{1/2} - 2^2S) = 14903.648 \text{ cm}^{-1}$  and  $E(2^2P_{3/2} - 2^2S) = 14903.983 \text{ cm}^{-1}$  [16]) and our experimental value of  $T_e$  in the C state (Table 2) we obtain the dissociation energy of the  $C^1\Pi_u$  state as  $7773.7 \pm 0.3 \text{ cm}^{-1}$ , where the uncertainty is mainly due to the estimated error of  $T_e$ . Thus the experimental potential curve provides reliable information on the molecular potential for about 57% of the well depth.

It is interesting to verify whether the IPA potential curve of the C state, constructed for the  ${}^7\text{Li}_2$  isotopomer, allows also to predict correctly positions of 30  $f$  parity rovibronic levels in the  ${}^6\text{Li}{}^7\text{Li}$  molecule observed in the present experiment. Taking into account a shift of the dissociation limit of the C state (equal to the isotope shift of  $2^2P - 2^2S$  atomic transition [16]), we find that the potential from Table 2 provides eigenenergies of levels in the  ${}^6\text{Li}{}^7\text{Li}$  isotopomer consistently too low by  $0.08 \pm 0.02 \text{ cm}^{-1}$ . This suggests a slight breakdown of the Born–Oppenheimer approximation for the  $\text{Li}_2$  isotopomers.

### 3.2. The $2^1\Sigma_u^+$ state

The recorded spectra of the  $2^1\Sigma_u^+ \leftarrow X^1\Sigma_g^+$  transition provided wave numbers of lines transformed to energies of 263 rovibrational levels of the  $2^1\Sigma_u^+$  state in the range  $30 \leq v' \leq 50$ ,  $3 \leq J' \leq 34$  (all of them corresponding to

the  ${}^7\text{Li}_2$  isotopomer). The data were supplemented with energies of 247 lower levels ( $0 \leq v' \leq 29$ ,  $8 \leq J' \leq 34$ ) from the previous experiment of Kasahara et al. [4] as well as additional 50 levels ( $0 \leq v' \leq 19$ ,  $3 \leq J' \leq 38$ ) from the measurements of Ross et al. [10]. Since the  $2^1\Sigma_u^+$  state corresponds to a double-well potential [1,4], it can be represented only by the potential energy curve built by a fully quantum-mechanical procedure such as the IPA method. However, analysis of this state requires a different strategy than presented in the previous subsection, because it contains only levels of  $e$  parity and a significant part of them can be perturbed due to the mutual  $2^1\Sigma_u^+ \sim C^1\Pi_u$  interaction. Therefore, we constructed the pointwise IPA potential using the robust fitting method proposed by Watson [17] which, in a given iteration of the fit, ascribes to a level  $i$  the weight defined as

$$w_i = \frac{1}{\sigma_i^2 + \alpha r_i^2}, \quad (2)$$

with  $\sigma_i$  is the experimental uncertainty,  $r_i$  is the residual from previous iteration and  $\alpha$  is a positive constant, which controls the influence of the residuals on corresponding weights. As a sensible starting point for the IPA routine and a reference for the initial determination of residuals, we used the experimental  $2^1\Sigma_u^+$  state potential of Kasahara et al. [4]. By trial and error we found that when setting  $\alpha = 0.5$  we obtain an optimum potential energy curve (Table 3 and Fig. 2) which is able to reproduce energies of all 560 observed rovibrational levels of the  $2^1\Sigma_u^+$  state with a standard error of  $0.25 \text{ cm}^{-1}$  and a dimensionless standard error of 0.85. To calculate energies of rovibrational levels, the potential should be interpolated using the natural spline algorithm [12] to generate a numerical mesh of at least 9000 points between 1.75 and 11.0 Å.

Table 3  
The IPA potential of the  $2^1\Sigma_u^+$  state in  ${}^7\text{Li}_2$

$R$ (Å)	$V$ ( $\text{cm}^{-1}$ )	$R$ (Å)	$V$ ( $\text{cm}^{-1}$ )
1.7	48950.8542	5.9	30413.1351
1.9	42065.4500	6.1	30400.3112
2.1	37081.6501	6.3	30445.3788
2.3	33999.3432	6.5	30539.6633
2.5	31989.5277	6.7	30676.6852
2.7	30817.7938	6.9	30849.1912
2.9	30252.4958	7.1	31046.7806
3.1	30101.6062	7.3	31277.5063
3.3	30230.2134	7.5	31539.8845
3.5	30542.4056	7.7	31799.8804
3.7	30966.8884	7.9	32030.2146
3.9	31446.5107	8.1	32264.4752
4.1	31916.4479	8.5	32763.4790
4.3	32257.2606	8.9	33262.9488
4.5	32229.5320	9.3	33745.9815
4.7	31868.8209	9.7	34200.3800
4.9	31496.7724	10.1	34610.8987
5.1	31171.6056	10.5	34988.4793
5.3	30900.7514	10.9	35297.1596
5.5	30668.3838	11.3	35564.0867
5.7	30498.0903		

The innermost and outermost points of the potential are again given mainly to enable numerical solution of the radial Schrödinger equation and the potential curve is reliable only between ca. 2.3 and 9.5 Å (that is up to an energy of about 34,000 cm<sup>-1</sup>). Still, the range of reliability has been extended by more than 1200 cm<sup>-1</sup> in comparison with the previous experimental work [4]. (A set of band-by-band constants related to this potential may be also found in [Supplementary material](#).) It must be noted that the constructed potential represents in the best way eigenenergies of the observed levels but is still open to further refinement requiring, however, full deperturbation of the  $2^1\Sigma_u^+ \sim C^1\Pi_u$  system.

#### 4. Comparison with theory

The experimental potential energy curves can be used to test the quality of the theoretical potentials of lithium dimer, recently published by Jasik and Sienkiewicz [1]. In [Fig. 2](#) both sets of curves corresponding to the  $C^1\Pi_u$  and  $2^1\Sigma_u^+$  states are drawn alongside, showing a striking similarity. For the C state the main difference, displayed in the inset, consists in position of the minimum of the potential, which is located by our experiment at internuclear distance larger than predicted theoretically by merely 0.004 Å and lower in energy by 76 cm<sup>-1</sup>. For the double minimum  $2^1\Sigma_u^+$  state the comparison is very favourable, too. The theoretical potential is only slightly deeper both in the inner and outer potential wells (by 59 and 92 cm<sup>-1</sup>, respectively) and the internal maximum shifted downwards by 31 cm<sup>-1</sup> comparing the experimental potential. The ordinates of the inner minimum ( $R_{\text{theor}} = 3.081$  Å vs  $R_{\text{exp}} = 3.094$  Å), the top of the potential barrier ( $R_{\text{theor}} = 4.374$  Å vs  $R_{\text{exp}} = 4.386$  Å) and the outer minimum ( $R_{\text{theor}} = 6.072$  Å vs  $R_{\text{exp}} = 6.040$  Å) also agree well. A more detailed comparison, in a form of  $R$ -dependent differences between the experimental and theoretical potentials, is given in the lower part of [Fig. 2](#). We conclude that calculations of Ref. [1] are capable of predicting properties of the  $C^1\Pi_u$  and  $2^1\Sigma_u^+$  states with high accuracy and similar precision can be expected for the results related to other medium

excited states of Li<sub>2</sub>. Nonetheless, experimental data are still superior in this field.

#### Acknowledgements

This work has been funded in part by the Polish Ministry of Science and Higher Education through Grant No. N202 103 31/0753. We thank Z. Jędrzejewski-Szmek for experimental assistance.

#### Appendix A. Supplementary data

Supplementary data associated with this article can be found, in the online version, at [doi:10.1016/j.chemphys.2007.02.001](https://doi.org/10.1016/j.chemphys.2007.02.001).

#### References

- [1] P. Jasik, J.E. Sienkiewicz, *Chem. Phys.* 323 (2006) 563.
- [2] X. Wang, J. Magnes, A.M. Lyyra, A.J. Ross, F. Martin, P.M. Dove, R.J. Le Roy, *J. Chem. Phys.* 117 (2002) 9339.
- [3] L. Li, S. Kasahara, Md.H. Kabir, Y. Sahashi, M. Baba, H. Katō, *J. Chem. Phys.* 117 (2001) 10805.
- [4] S. Kasahara, P. Kowalczyk, Md.H. Kabir, M. Baba, H. Katō, *J. Chem. Phys.* 113 (2000) 6227.
- [5] W. Jastrzębski, P. Kowalczyk, *Phys. Rev. A* 51 (1995) 1046.
- [6] A. Grochola, W. Jastrzębski, P. Kertyka, P. Kowalczyk, *J. Mol. Spectrosc.* 221 (2003) 279.
- [7] I. Shoshan, N.N. Danon, V.P. Oppenheim, *J. Appl. Phys.* 48 (1977) 4495.
- [8] P. Kusch, M.M. Hessel, *J. Chem. Phys.* 67 (1977) 586.
- [9] M.M. Hessel, C.R. Vidal, *J. Chem. Phys.* 70 (1979) 4439.
- [10] A.J. Ross, P. Crozet, C. Linton, F. Martin, I. Russier, A. Yiannopoulou, *J. Mol. Spectrosc.* 191 (1998) 28.
- [11] A. Pashov, W. Jastrzębski, P. Kowalczyk, *Comput. Phys. Commun.* 128 (2000) 622.
- [12] C. DeBoor, *A Practical Guide to Splines*, Springer, Berlin, 1978.
- [13] A. Pashov, W. Jastrzębski, P. Kowalczyk, *J. Chem. Phys.* 113 (2000) 6624.
- [14] W.T. Zemke, W.C. Stwalley, *J. Phys. Chem.* 97 (1993) 2053.
- [15] J.A. Coxon, T.C. Melville, *J. Mol. Spectrosc.* 235 (2006) 235.
- [16] C.J. Sansonetti, B. Richou, R. Engelman Jr., L.J. Radziemski, *Phys. Rev. A* 52 (1995) 2682.
- [17] J.K.G. Watson, *J. Mol. Spectrosc.* 219 (2003) 326.